



ELSEVIER

Computers and Electronics in Agriculture

34 (2002) 173–190

Computers
and electronics
in agriculture

www.elsevier.com/locate/compag

Experimental and numerical studies on the heterogeneity of crop transpiration in a plastic tunnel

T. Boulard ^{a,*}, S. Wang ^b

^a *Unité Plantes et Systèmes Horticoles, I.N.R.A., Site Agroparc, 84914 Avignon, Cedex 9, France*

^b *Department of Biological Systems Engineering, Washington State University, 213 L.J. Smith Hall, Pullman, WA 99164-6120, USA*

Abstract

The heterogeneity of crop transpiration is important to clearly understand the microclimate mechanisms and to efficiently handle the water resource in greenhouses. A computational fluid dynamic software (CFD2000) was used to study the climate and crop transpiration distributions in a $22 \times 8 \text{ m}^2$ plastic tunnel situated in Avignon, France, together with a global solar radiation model and a crop heat exchange model. The distribution of solar radiation within the greenhouse tunnel was determined based on the path of the sun, the greenhouse geometry, the cover transmittance and the sky conditions. The crop transpiration was deduced by assimilating the crop to a porous medium exchanging latent and sensible heats with its environment. The radiative and convective heterogeneity in two vertical sections of the tunnel predicted by the CFD model was validated against the experimental results obtained by a group of solar cells and sonic anemometers. The validated model was finally used to predict the transpiration flux of a mature lettuce crop in the tunnel. The crop transpiration strongly varied (up to 30%) according to the place in the tunnel. The predicted crop transpiration was in close agreement with the measured value both along the sections with the side openings and between the consecutive openings. © 2002 Elsevier Science B.V. All rights reserved.

Keywords: Greenhouse tunnel; Crop transpiration; Climate heterogeneity; CFD

* Corresponding author. Tel.: +33-4-3272-2285; fax: +33-4-3272-2282.

E-mail address: boulard@avignon.inra.fr (T. Boulard).

1. Introduction

Greenhouse tunnels are widely used in the whole world due to their low cost, simple structure and easy management. However, spatial heterogeneity of airflow, air temperature and humidity vary strongly in these structures and the heterogeneity of crop transpiration is marked. Therefore, quantitative understanding of this heterogeneity can help growers to optimise fertilisation and irrigation systems and solve environmental problems, such as, the over-consumption of irrigation water and the loss of nitrogen to the environment.

The ventilation process is the driving force for the airflow distribution, climate and crop transpiration heterogeneity in greenhouses (Bot, 1983; De Jong, 1990; Fernandez and Bailey, 1992; Boulard and Draoui, 1995; Boulard et al., 1996). The inside solar radiation distribution is one of the important factors for the crop transpiration (Wang and Boulard, 2000a). Several studies on natural ventilation were based on estimations of a global air exchange rate (Boulard and Baille, 1995; Kittas et al., 1995) and simulations of a homogeneous air temperature and a global vegetation temperature using a big leaf model (Stanghellini, 1987; Yang et al., 1990; Boulard and Wang, 2000) and energy balance methods (Kindelan, 1980; de Halleux et al., 1991; Wang and Deltour, 1996). However, these methods do not allow to clearly map airflow patterns, temperature profiles and heterogeneity of the crop cover transpiration. Meanwhile, some progress in flow modelling by computational fluid dynamics (CFD) (Mistriotis et al., 1997) and in airflow measurements has recently been made for a closed greenhouse (Boulard et al., 1998), a two-span naturally ventilated greenhouse (Boulard et al., 1997; Wang et al., 1999), a multi-span sawtooth greenhouse (Kacira et al., 1998) and a multi-span Venlo-type greenhouse (Wang and Deltour, 1999). Recently, a radiative distribution model was developed for predicting the solar radiation heterogeneity within the greenhouse tunnel, based on path of the sun, the greenhouse geometry, the cover transmittance and sky conditions (Wang and Boulard, 2000b). Up till now, very few studies on the detailed climate heterogeneity in full-scale greenhouses including a crop cover have been conducted by both experiments and modelling.

The objectives of this study were to combine solar radiation and crop transpiration models with the commercial CFD software (CFD2000); to validate the predicted radiative and convective heterogeneity by the experimental values obtained by solar cell and sonic anemometer systems; to simulate the heterogeneity of transpiration of a lettuce crop in the tunnel based on the sensible and latent heat exchanges with its environment; and to compare the predicted crop transpiration distribution with the experimental value obtained by micro-lysimeters.

2. Materials and methods

2.1. Experimental set-up

2.1.1. Site and tunnel description

The experimental plastic tunnel (22×8 m²) was located in Avignon (44°N

latitude, 5°E longitude and 24 m altitude), in the south of France. It was covered with a polyethylene sheet and the averaged measured transmittances in the tunnel centre was equal to 0.53 in cloudy conditions and 0.56 in sunny conditions. Traditional discontinuous vent openings were made by separating plastic sheets every 4 m along both sides of the tunnel. A schematic view of the experimental tunnel is shown in Fig. 1. Since this region is characterised by a predominant northerly wind, channelled by the Rhône valley, symmetric airflow was assumed along the v direction with respect to each opening. Therefore, two transverse sections were selected to explore the flow patterns. A ‘vent’ section (II) was situated in the middle of the central vent openings and a middle section (I), placed at 2 m westward from the section II.

2.1.2. Measurement systems

The experiments used to validate the simulations were performed in the same greenhouse tunnel in three steps: (i) the air flow, temperature and humidity patterns used to validate the fluid dynamics model were first measured in October 1997; (ii) the solar radiation distribution used to validate the radiative heterogeneity model was measured in February and March 1999; and (iii) the lettuce crop transpiration distribution used to validate the global model integrating the radiation and transpiration models with the fluid dynamics model was measured in March 1999. We shall summarise the main characteristics of the steps (i) and (ii) which have already been published and give further details of step (iii) which has not been yet presented.

2.1.3. Convective measurements

External air speed and temperature were measured by two three-dimensional (3D) sonic anemometers (R3, Gill Solent, UK) and air humidity by two krypton

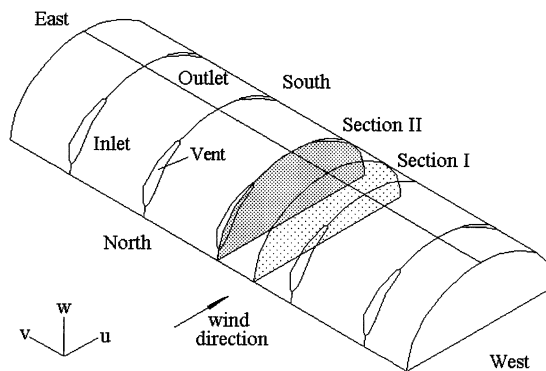


Fig. 1. Schematic view of the experimental plastic (polyethylene) tunnel ($22 \times 8 \text{ m}^2$). (u , v and w are three components of the air velocity measured by the sonic anemometer in two sections).

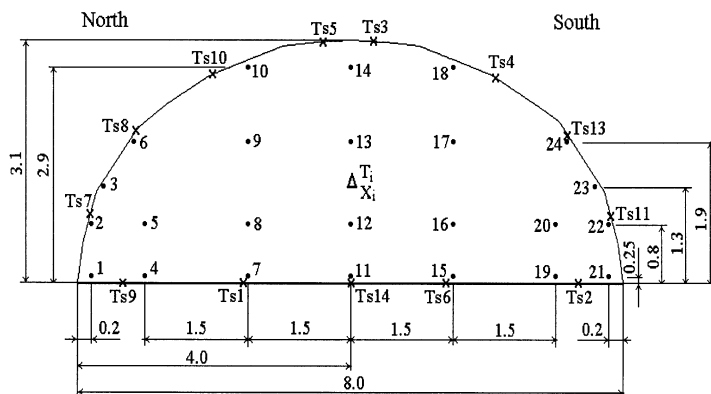


Fig. 2. Measurement positions in the central section of the tunnel. All dimensions are in metres (m). (●) Air temperature, humidity and velocity (1–24); (×) surface temperature ($T_{s1} - T_{s14}$); (Δ) reference inside air temperature and humidity measurements (T_i, X_i).

hygrometers (K-H₂O, Campbell Scientific Ltd, USA) in 5 Hz frequency. These four instruments were moved from one place to another at 48 positions for the two sections (Fig. 2). The measurement process for 5 min data collections each two positions took several hours on 24 October 1997. With only two sampling positions possible at any one time, a difficulty arises from how to deal with changing external conditions throughout the time needed to measure the 24 different measurement positions within each cross section. This problem was overcome:

- (i) by selecting measurements for a fixed northerly external wind direction, and
- (ii) by using an external reference wind speed U_o and the difference in air temperature ($T_i - T_o$) and humidity ($X_i - X_o$) between the centre of the greenhouse (subscript i) and the external airstream (subscript o) as scaling parameters.

In this way, the influence of external climatic conditions on the experimental data was reduced by normalisation. Surface temperatures at 14 positions along the soil surface and the plastic cover surface were also measured by means of thin thermocouples. More details on the experimental procedure and on the mean and turbulent air flows and microclimatic patterns resulting of these experiments can be found in Boulard et al. (2000).

2.1.4. Radiative measurements

The solar radiation distributions were measured by 32 silicon solar cells disposed along four sections on the soil surface in the middle of the tunnel on 25 February and 21 March 1999. Two of the test sections were located at the same places as shown in Fig. 1. A complete description of the measurement instruments and of the procedure can be found in Wang and Boulard (2000b). The global solar transmit-

tance distributions over these two sections (II and I) were used to validate the radiative heterogeneity model. During this second experiment (March 1999), the transpiration heterogeneity was also determined. As the experimental design and the results of these measurements were not yet published, they will be presented before being used to validate the complete model combining the radiative heterogeneity model and the crop transpiration heterogeneity model with the CFD software.

2.1.5. Crop transpiration measurement

During the transpiration measurements, the external wind speed and direction were measured by a cup anemometer and a wind vane situated 1 m above the greenhouse. Interior and exterior air temperatures and humidities were also measured by ventilated thermometers/psychrometers situated in the centre and 1 m away from the greenhouse at a height of 3 m. The external global and diffuse solar radiations were detected near the tunnel using pyranometers fixed on a mast at 3 m height. All the measurements were sampled each 10 s and averaged online over 10 min, then stored in a portable data logger (DELTA-T, Cambridge, UK). Table 1 provides the mean external (and internal) climate conditions during the crop transpiration experiments which were also used as boundary conditions for the simulation of the global model combining the models of heterogeneity of the inside solar radiation and crop transpiration with the CFD software.

The two-dimensional transpiration flux of a mature lettuce crop was measured on 23 and 24 March 1999 using micro-lysimeters supporting lettuces. The heterogeneity of crop transpiration was investigated by weighing along the ‘vent’ section (II) situated in the middle of the center vent openings and along the middle section (I) situated between two openings (Fig. 1). Six micro-lysimeters were uniformly installed for each section. The lysimeters consisted of a plastic cylinder with 152 mm internal diameter and 180 mm long and were inserted into an outer cylinder. They were filled with soil and closed off at the bottom by a grille enabling water exchanges with layers below to take place. There was only one lettuce in each micro-lysimeter and the transpiration rate of each plant during the period t_1-t_0 was determined using gravimetry, as follows:

Table 1
Mean climatic conditions during the day for crop transpiration measurement

Parameters	23 March	24 March
External wind speed (m s^{-1})	1.6	0.9
Outside air temperature ($^{\circ}\text{C}$)	10.9	12.7
Inside air temperature ($^{\circ}\text{C}$)	13.0	16.0
Outside air humidity (%)	47.2	58.9
Inside air humidity (%)	51.2	63.8
Global solar radiation (W m^{-2})	407	392
Diffuse solar radiation (W m^{-2})	66	84

$$\lambda E = \frac{[w(t_1) - w(t_0)]}{A_0(t_1 - t_0)} \quad (1)$$

where A_0 is the internal area of the lysimeter (m^2), t_1 and t_0 are the measurement time (s), w is the mass (kg), λ is the latent heat of water vaporisation (J kg^{-1}) and λE is the crop transpiration flux (W m^{-2}). The measurements were performed every 3 h during the diurnal period and the crop transpiration at each location was accumulated and averaged over the measurement period. The weighing accuracy was ± 10 g and was equivalent to ± 5 g m^{-2} of crop transpiration. In addition, the leaf area index was estimated during the experiment from measurements of leaf dimensions (non-destructive measurements) and from the correlation between the width and length of the leaves and their surface area (destructive measurements).

2.2. Simulation

2.2.1. Solar radiation

The global solar radiation contributes to a large part of crop transpiration in greenhouses. The transmission of solar radiation into a plastic tunnel is influenced by radiative properties of the cladding material, effects of structure (frames, vent openings, side walls and gable ends) and sky conditions. For the simplicity of this model, continuous curved surfaces of the arched tunnel were approximated by a limited number of small flat planes. The second reflections from inner cover surfaces and from the soil surface were neglected. With these assumptions, a bundle of global solar radiation transmitted through a given surface was calculated and projected according to a 'shadow area' on the soil surface (Wang and Boulard, 2000b):

$$S_g(x', y', z') = \tau_D \cdot S_D + \tau_d \cdot S_d \quad (2)$$

where x' , y' and z' are the Cartesian co-ordinates for the positions at the cover surface, S_d and S_D are the external diffuse and direct solar radiations (W m^{-2}), $S_g(x', y', z')$ is the internal global solar radiations (W m^{-2}), τ_d and τ_D are the solar diffuse and direct transmittances of the elementary surface of the tunnel. For further simplifying the model, it is assumed that the light transmissivity is zero for tunnel frames and 1 for vent openings. The experimental value of the transmissivity of the plastic cover was defined as a function of the incidence angle α in rad, which is a function of the solar height angle γ (rad), the solar azimuth ψ (rad) and the angle of orientation of an elementary plane of the cover θ (rad). If the origin of the co-ordinate system is assumed at north-east corner of the tunnel, the position (x , y) that the solar beam reached on the soil surface can be determined as follows (Wang and Boulard, 2000b):

$$\begin{aligned} x &= \frac{x' + z' \cos \psi}{tg\gamma} \\ y &= \frac{y' - z' \sin \psi}{tg\gamma} \end{aligned} \quad (3)$$

Table 2

Reduced form of the variables, concentration Φ , diffusion Γ , and source S_Φ terms, of the mass, momentum and energy conservation equations (CFD2000 manual, 1997)

	Φ	Γ	S_Φ
Mass	1	0	0
Momentum (X)	$U = u/V_0$	$1/Gr^{0.5}$	$-\partial P/\partial X$
Momentum (Y)	$V = v/V_0$	$1/Gr^{0.5}$	$-\partial P/\partial Y$
Momentum (Z)	$W = w/W_0$	$1/Gr^{0.5}$	$\theta \cdot \partial P/\partial Z$
Energy	$\theta = (T - T_0)/\Delta T$	$1/PrGr^{0.5}$	0

P , pressure term; θ , temperature ratio; $T, T_o, \Delta T$, temperature inside, outside, and step; U, V and W , three components of velocity vectors; u, v and w , three components of air speeds; V_0 , outside air speed; X, Y and Z , co-ordinates; Gr and Pr , Grashof and Prandl numbers, respectively.

The solar radiation distribution in the sections II and I was predicted by inputting the external global solar radiation and diffuse solar radiation at the same day as taken for the experiment. The detailed description of the model was described elsewhere (Wang and Boulard, 2000b).

2.2.2. Fundamental computational aerodynamics

The fundamental calculation of the airflow pattern is based on computational aerodynamics, which uses the mass, momentum and energy conservation equations. For an incompressible fluid, the three-dimensional conservation equations describing the transport phenomena for steady flows in free convection are of the general form (CFD2000 manual, 1997):

$$\frac{\partial(U\Phi)}{\partial X} + \frac{\partial(V\Phi)}{\partial Y} + \frac{\partial(W\Phi)}{\partial Z} = \Gamma \cdot \nabla^2\Phi + S_\Phi \tag{4}$$

where Φ represents the concentration of the transported quantity in a non-dimensional form, namely the three-dimensional momentum (Navier–Stokes) and the scalar mass and energy conservation equations; U, V and W are the components of velocity vector; Γ is the diffusion coefficient; and S_Φ is the source term. These variables, with their diffusion, Γ and source terms, S_Φ , are shown in Table 2. These equations of partial differential form are highly non-linear. The numerical codes known as Computational Fluid Dynamics codes (CFD) using a spatial discretisation were necessary for solving the set of equations described by Eq. (4) and Table 2 which gives the flow characteristics on a finite domain spanned by a grid.

As shown by the measurements of turbulent air flows and microclimatic patterns in a greenhouse tunnel (Boulard et al., 2000), the air flows were highly turbulent. Consequently, turbulence models must be introduced in the Reynolds equations written to separate the mean flow from its fluctuating components. One of the most widely used closure procedures is the $k-\epsilon$ model (Launder and Spalding, 1974) which introduces two new phenomenological variables: the turbulent kinetic energy k , and its dissipation rate ϵ . The set of transport equations established in laminar regime remains valid and the transport equations of k and ϵ must also be

considered in the form of Eq. (4). The complete set of the equations of the $k-\varepsilon$ model can be found in Mohammadi and Pironneau (1994) and their commonly used set of parameters (empirically determined) are given in CFD2000 manual (1997).

The sink of momentum due to the drag effect of the crop, is symbolised by the source term S_ϕ of the Navier–Stokes equation Eq. (4). This drag force may be expressed by unit volume of the cover by the commonly used formula (Wilson, 1985):

$$S_\phi = -L C_D v^2 \quad (5)$$

where v is the air speed, L the leaf area density ($\text{m}^2 \text{m}^{-3}$) and C_D a drag coefficient. For a mature greenhouse tomato crop, Haxaire (1999) found $C_D = 0.32$ using wind tunnel facilities.

In order to include the drag effect proportional to the leaf density into our CFD study, the crop cover was considered as a porous medium and the Darcy–Forseheimer equation was used (CFD2000 manual, 1997):

$$S_\phi = -\left(\left(\frac{\mu}{K}\right)v + \left(\frac{C_F}{K^{0.5}}\right)v^2\right) \quad (6)$$

where μ is the dynamic viscosity of the fluid, K the permeability of the porous medium and C_F the non-linear momentum loss coefficient.

For the range of air speed observed into the crop cover, the term in v of Eq. (6) can be neglected in front of the quadratic term. The non-linear momentum loss coefficient C_F and the permeability K of the medium can be deduced from the combination of Eq. (5) and Eq. (6) through the following relation:

$$\frac{C_F}{\sqrt{K}} = LC_D \quad (7)$$

2.2.3. Commercial computational fluid dynamic package

A commercial solver software: CFD2000[®] (CFD2000 manual, 1997) made it possible to obtain the numerical solution by use of a finite volume discretisation code and the pressure implicit with splitting of operators (PISO) algorithm developed by Issa (1985). The driving force of the natural convection is the buoyancy force arising from small temperature differences within the flow according to the Boussinesq hypothesis. A standard equation $k-\varepsilon$ model assuming isotropic turbulence was used to describe the turbulent transport, this choice being a good compromise for a realistic description of turbulence and computational efficiency (Jones and Whittle, 1992).

2.2.4. Mesh and boundary conditions

With the wind direction perpendicular to the axis of the tunnel, the problem of the transfers in the middle of the tunnel can be considered as a periodic problem requiring only the study of one period. Limits of the computational domain included one period of the tunnel centred on one pair of openings with the walls, soil surface and one inlet and one outlet as boundaries.

The measured air velocity, temperature and humidity profile in the windward opening were taken as boundary condition and the measured temperatures were applied to all wall boundaries (Fig. 2) and outlet boundary conditions were automatically computed to satisfy the continuity conditions. The inlet velocity, temperature and humidity were taken from the experimental values from October 1997 and March 1999 to validate successively the fluid dynamics model alone (without the modelling of crop transpiration), and the global model, incorporating the crop transpiration model.

In order to study the air flow in the whole tunnel and the effects of the gable ends, a special simulation of the flow exchanges excluding thermal and water vapour transfers, was also performed on the whole 22 m tunnel (Fig. 1).

The computational grid of the CFD software used Cartesian co-ordinates and a finer resolution was imposed in critical portions of the flow subject to strong gradients (wall boundary layers and the mixing regions). Body fitted co-ordinates were also applied to exactly conform the grid to the contours of the boundary conditions. After several tries with different densities, the calculations were based on a $32 \times 20 \times 64$ grid. It results from an empirical compromise between a dense grid, associated with a long computational time, and a less dense one, associated with a marked deterioration of the simulated results.

2.2.5. *The porous medium*

The porous medium approach described by Eq. (6) and available in the CFD software (CFD2000 manual, 1997) was used to model the dynamic effect of the crop cover on the flow. For the lettuce crop considered in our simulation, we have neglected the head of the lettuce which does not participate to the flow transfer (nor to the transpiration) and we have considered an 'effective' (with respect to transpiration) leaf area index equal to 5. The parameters K and c_F involved in Eq. (6) were deduced from Eq. (7) with $C_D = 0.32$ (Haxaire, 1999) and $L = 0.25$. The following values: $K = 1$, and $c_F = 0.08$ were deduced and used in relation with Eq. (6) to model the dynamics of air within the porous medium corresponding to the limits of the crop cover (0.2 m high on all the surface of the greenhouse).

2.2.6. *The model of crop transpiration*

The interposition of a crop cover in airflow gives rise to a sink of momentum. Likewise, the absorption of solar energy by the leaves is accompanied by sensible and latent (crop transpiration) heat exchanges between the crop cover and the air. All these aspects were considered in conjunction with the use of CFD.

The exchange of heat and water vapour between leaves and air was considered through the heat and mass balance of leaves with the air. Each mesh of the crop cover was assimilated to a 'volumic heat source boundary condition' receiving a radiative flux which was deduced from the radiative transfer model described before (Wang and Boulard, 2000b). This flux was partitioned into convective sensible and latent heat fluxes (water vapour) depending on the heat and water exchanges (stomatal and aerodynamic) between a virtual solid matrix representing the cover and characterised by its surface temperature and the air (Haxaire, 1999).

$$R_n - \frac{\rho C_p L_{ai}(T_l - T_a)}{r_a} - L_{ai} \rho \lambda \frac{w_f - w_a}{r_a + r_s} = 0 \quad (8)$$

where C_p is the specific heat of air at constant pressure ($\text{J kg}^{-1} \text{K}^{-1}$), r_a is the aerodynamic resistance of the leaf (s m^{-1}), r_s is the stomatal resistance of the leaf (s m^{-1}), L_{ai} is leaf area index, T_l and T_a are leaf and air temperatures ($^{\circ}\text{C}$), w_f and w_a are the absolute humidity of the leaf and the air (kg per kg), and ρ is the air density (kg m^{-3}). In Eq. (8), the first term represents the net radiation (R_n , W m^{-2}), the second term represents the sensible heat exchange and the third term the latent heat exchange (crop transpiration).

Following Campbell (1977), if the interior air speed $v < 0.1 \text{ m s}^{-1}$, then:

$$r_a = 840 \left(\frac{d}{|T_l - T_a|} \right)^{0.25} \quad (9)$$

else:

$$r_a = 220 \frac{d^{0.2}}{v^{0.8}} \quad (10)$$

where d is the characteristic length of the leaf (m), and v is the air speed at the given location (m s^{-1}). The stomatal resistance was adopted from Pollet et al. (1999):

$$r_s = \frac{200(31 + S_g) [1 + 0.016*(T_a - 16.4)^2]}{(6.7 + S_g)} \quad (11)$$

where S_g is the global solar radiation at the given location (W m^{-2}).

The CFD program was customised in FORTRAN in order to perform the balance described by Eq. (8) and Eqs. (9)–(11), based on the local computed air speed and climatic conditions within each mesh of the porous medium (crop cover). It follows that two additional outputs of great interest were available for each mesh of the crop cover: the temperature of the crop surface T_l and the transpiration of the cover:

$$\lambda E = L_{ai} \rho \lambda \frac{w_f - w_a}{r_a + r_s} \quad (12)$$

2.2.7. Recapitulative of the different operations

A recapitulative of the different operations is as follows:

- (i) In the first step, the radiative model allowed for determination of the solar energy arrives at the soil level on each mesh of the crop cover (assimilated to a porous medium in the CFD model) and was assimilated to a ‘heat source boundary condition’. At the same time, the airflow pattern and climate heterogeneity were predicted by the CFD software including also the description of the crop cover as a porous medium. The inputs describing the mean external climate conditions are listed in Table 1.
- (ii) In the second step, the solar energy absorbed by the crop was partitioned into convective sensible and latent heat fluxes (water vapour) using the customised CFD and modelling the fluid dynamics together with the energy and water

vapour transfers at crop level described by Eqs. (8)–(11). This partition depended on the heat and water vapour exchanges (stomatal and aerodynamic) between the solid matrix of the porous medium and the air within each mesh of the porous medium. These stomatal and aerodynamic resistances relied on the computed air speed and climatic conditions and the resulting water vapour flux Eq. (12) constituted the crop transpiration flux.

3. Results and discussion

3.1. Model validation

3.1.1. Solar radiation

The comparison between measurements and simulations was carried out based on the measurements performed along the two sections (II and I) in the centre of the tunnel. Daily averaged transmittances in the centre of the tunnel under a clear sky are shown in Fig. 3. For both sections, the transmittance was clearly higher on the south part of the tunnel and lower near the south and north borders due to larger incidence angles. It has also to be noticed that no differences of transmissivity were detected for the surfaces situated on the south side just below the openings (section II) and the similar positions situated in the middle of two successive openings below the cover (section I). On average, transmittance variations as a function of the tunnel width obtained by experiments and simulations fitted well.

3.1.2. Airflow and temperature patterns

Fig. 4 shows the normalised air velocity distributions (in %) obtained by CFD simulation in sections I and II, with $U^* = 100\%$ corresponding to the module of the outside wind speed. The normalised air velocity was obtained by the ratio of the interior air velocity to the mean external wind speed. It was observed that the

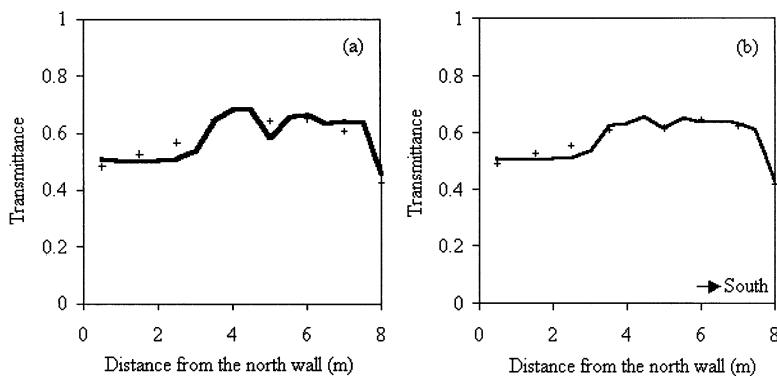


Fig. 3. Measured (+) and calculated (—) daily averaged transmittances of the global solar radiation in the centre of the tunnel along sections II (a) and I (b) under clear sky conditions (25 February).

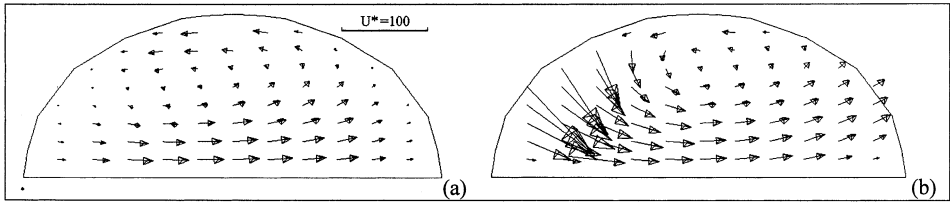


Fig. 4. Normalised air velocity (U^*) distributions obtained by simulation in sections I (a) and II (b).

airflow pattern in the vent opening section (section II) was characterised by a strong airflow entering through the northern opening, crossing the tunnel and then outgoing through the southern opening. However, the air speed was much weaker in section I centred between two consecutive openings. The simulated air speed (Fig. 5) seemed to be larger than the measured value because the averaged experimental air velocity was taken by neglecting its turbulent part. Considering the air circulation in section II, the mass conservation was not demonstrated due to the inflow exceeding the outflow. In fact, the lateral air circulation was not symmetric with respect to the middle of each vent opening. The air speeds reached maximum value (100%) at the air inlet, 30% in the air outlet and null in the border of the tunnel in section I. A similar airflow pattern was obtained between the measurement and simulation as shown in Fig. 5.

The normalised temperature fields in sections I and II are shown in Fig. 6. The normalised value was obtained by the ratio of the temperature difference between

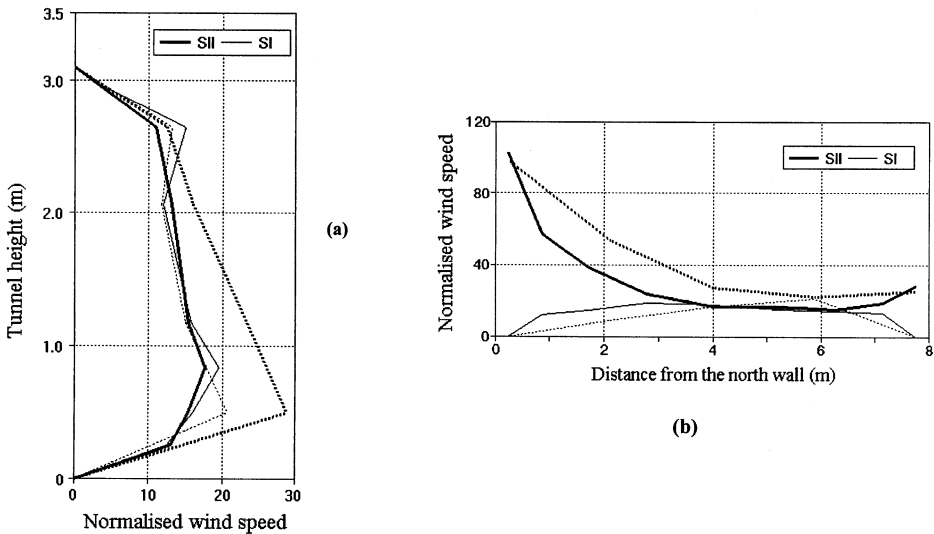


Fig. 5. Normalised air speed (expressed in % of outside wind speed) obtained by simulation (----) and measurement (—) in the middle (a) and at 1 m height (b) of the tunnel. SII and SI indicate the sections with the openings and between two consecutive openings, respectively.

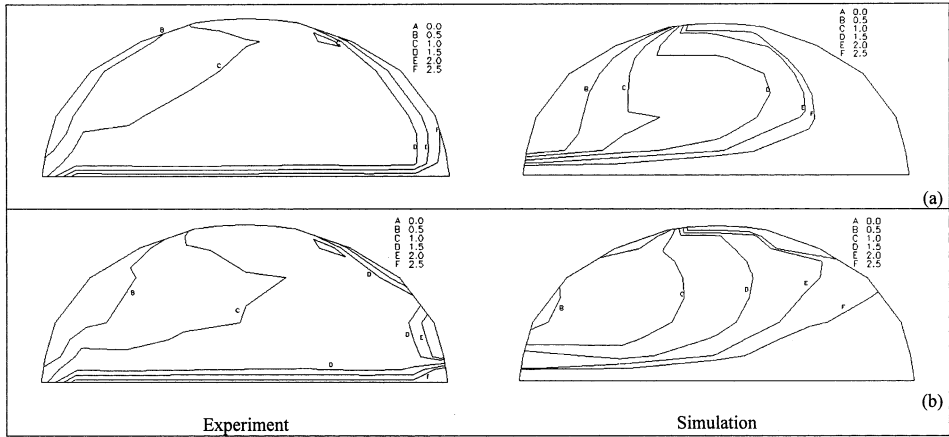


Fig. 6. Distribution of the normalised air temperature difference between inside and outside obtained by experiment and simulation in sections I (a) and II (b), respectively.

each point and outside to the difference between inside (in the middle of the tunnel at 1m high) and outside (2.2 °C). Generally, section I was slightly warmer than section II because of the cold air penetration into this section. A strong north to south gradient was obtained in section II. In the north opening and along the north side of the tunnel in section I, the air temperature was close to the outside value (only 0.5 °C more). In contrast, the areas situated along the south side and near the south opening of the tunnel were significantly warmer (1.5–2.5 °C). Solar radiation absorption at the soil surface also generated a strong gradient (1.5–2.5 °C) in the first 20 cm above the soil surface. An acceptable agreement was achieved for temperature fields between measurement and simulation both in the two sections.

3.2. Model applications

3.2.1. Solar radiation distribution

Fig. 7 illustrates the averaged (between sunset and sundown) global solar radiation distribution predicted by the solar radiation model over the ground surface of the full-scale tunnel on March 21, for clear sky conditions. Considerable variations of the global solar radiation in the tunnel were observed. The higher values of the solar radiation were due to the effect of vent openings, and the lower values were caused by larger angles of incidence of solar radiation. Larger heterogeneity was observed along the transversal section of the tunnel, due to low sun's position. However, higher contrasts were found between the areas with a high transmittance situated below the vent openings and in the middle of the tunnel, and the zones with a low transmittance situated along the sides and gable ends. Along the sections II and I in the center of the tunnel, the radiative intensity was higher on the south side than on the north side (about 30% more) because the solar radiation directly entered through the openings and, in March, the incidence angle at low parts of the tunnel cover was smaller than that at high parts.

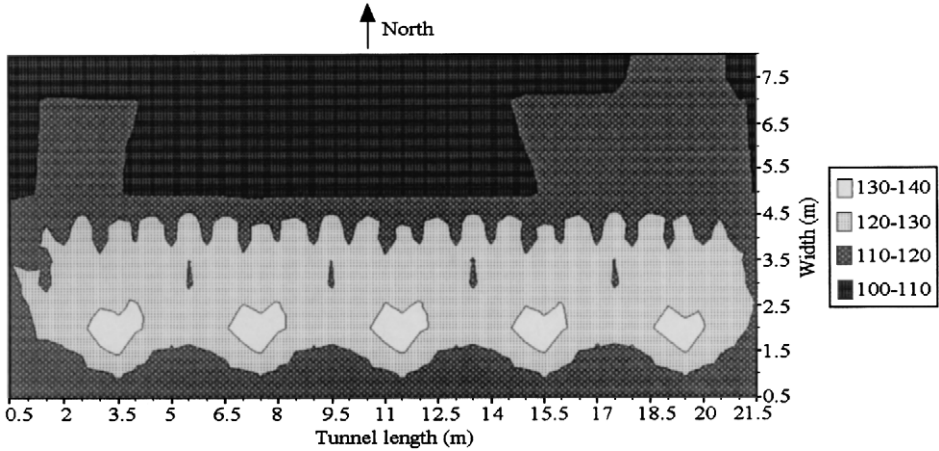


Fig. 7. Simulated average (on the diurnal period) solar radiation distribution in E–W oriented tunnel on 21 March under clear weather conditions. The outside average solar radiation was $196 W m^{-2}$. The unit of solar radiation is in $W m^{-2}$.

3.2.2. Airflow pattern

Fig. 8 shows the airflow pattern at 1 m height obtained by CFD simulation in the full scale tunnel. It confirms the periodic character of the flow pattern characterised by a strong transverse current at the level of each serial of openings. However, it stresses that the lateral air circulation was not exactly symmetric with respect to the center of each opening, particularly for the openings situated near the two extremities of the tunnel and the occurrence of a general North–West to South–East current.

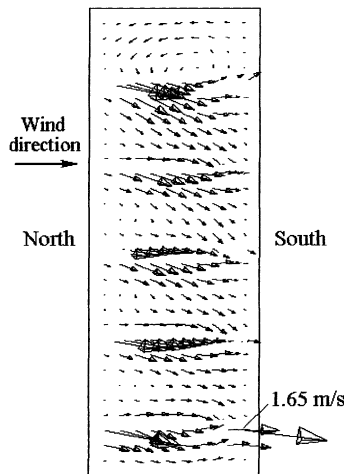


Fig. 8. Simulated airflow pattern at 1 m height in the full-scale tunnel.

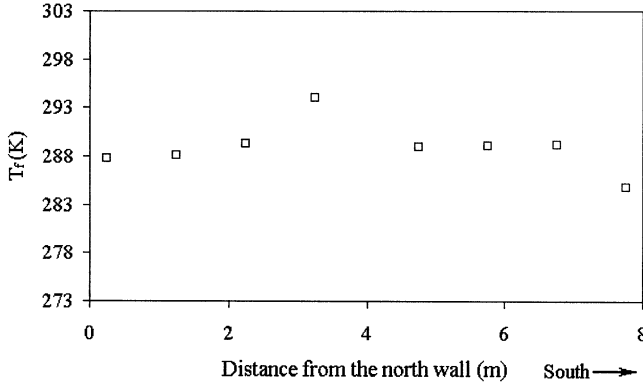


Fig. 9. Predicted lettuce leaf temperature (K) simulated along the section with the openings on 23 March.

3.2.3. Crop transpiration

Crop transpiration distributions depend on both the solar radiation intensity and convective exchange distributions together with the influence of inside climate heterogeneity on the stomatal and aerodynamic resistances. Fig. 9 shows the lettuce leaf temperature distribution simulated in the section with the openings. The leaf temperature was a function of global solar radiation, aerodynamic and stomatal resistances (Fig. 10). The computed aerodynamic resistance of the lettuce leaves took into account mainly the air speed at crop level and temperature differences between the leaf and the interior air according to natural and forced ventilation types. The highest value near the middle of the tunnel was caused by small air speed in forced convection and the smallest value closed to the south cover of the tunnel was caused by natural convection, as shown by the leaf temperature elevation at the same level (Fig. 9). The computed stomatal resistance of lettuce leaves (Fig. 10b) did not vary along the section because it only varied with the absorbed solar radiation of the leaves in which the difference was small at different positions along the section.

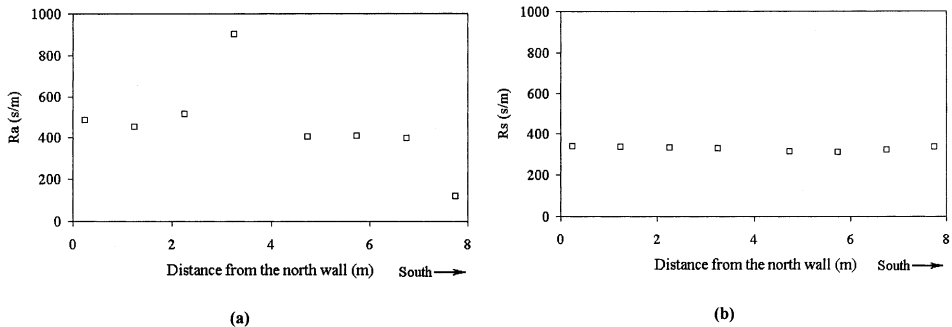


Fig. 10. Distribution of the computed aerodynamic (a) and stomatal (b) resistances of the lettuce leaves along the section with the openings on 23 March.

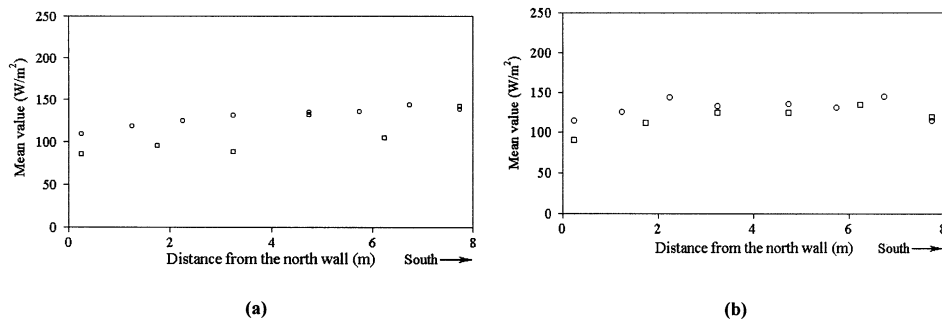


Fig. 11. Distribution of the computed (○) and measured (□) transpiration of the lettuces along the section with the openings (a) and along the section between the consecutive openings (b) on March 23.

The resulted distributions of crop transpiration from simulation and measurement are presented in Figs. 11 and 12, respectively, for March 23 and 24 for the section with the openings and the section between the consecutive openings. For both days, the computed and measured values of crop transpiration on the south were higher than in the centre and north because of the larger solar radiation received on the south side due to direct entering. The discrepancy between the measured and calculated values of transpiration was more important in the section with the openings, particularly in the middle of the tunnel, with systematically smaller measured values than calculated. However, the predicted and experimental values were generally similar along the section between the openings, and both values of crop transpiration on the north side were about 30% lower than other locations because of lower air speed and solar radiation. If the validation of the model is satisfactory in the section without openings, the divergences observed in the section subject to higher solar and convective fluxes might be due to either a stomatal regulation, because of the importance of the atmospheric demand, or a reduction of the leaf area index in this zone, because of the same cause, or even a combination of these two causes. However, these regulations due to the biology of the plants were not considered in the model and they appeared as being the major

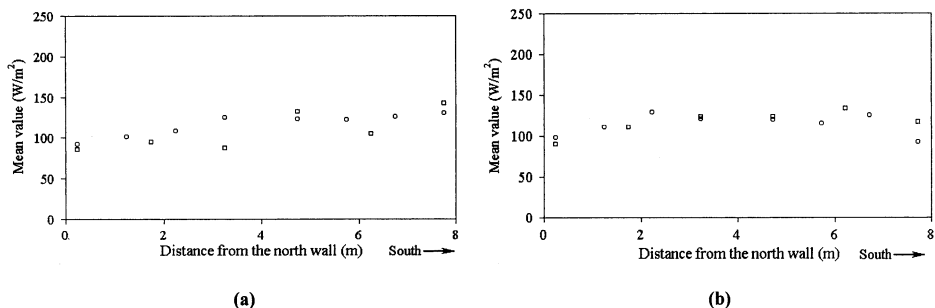


Fig. 12. Distribution of the computed (○) and measured (□) transpiration of the lettuces along the section with the openings (a) and along the section between the consecutive openings (b) on 24 March.

limitation of this approach only based on the atmospheric demand without any other limitations.

4. Conclusions

1. The study of solar radiation distribution, airflow patterns, temperature and humidity fields generated by tunnel structures, wind and buoyancy forces in a full-scale naturally ventilated tunnel can be performed by the customisation of a CFD software in order to consider also the radiative transfers and the transpiration of the crop cover.
2. Comparisons of measurements and modelling show acceptable agreements between the measured solar radiation, airflow and temperature distributions and the simulated results. The computational fluid dynamics software can be effectively used to predict the greenhouse air circulation.
3. The climate heterogeneity was characterised by a strong crossing flow from windward to leeward openings, while the air along the floor and walls stayed still, particularly at crop level for a culture like lettuce (near the soil surface). Strong temperature gradients from north to south and above the soil surface were observed due to the cold air penetration and solar energy absorption at the soil surface, respectively. The humidity gradient was mainly concentrated along the soil surface due to water evaporation from the lettuce crop.
4. The predicted crop transpiration was in good agreement with the measured value and both approaches demonstrated that crop transpiration on the north side was about 30% smaller than other locations because of lower solar radiation and air speed.

CFD can, therefore, be a very useful tool in the study of the heterogeneity of internal greenhouse climate and crop transpiration. The model being validated, many aspects which influence the internal climate (e.g. vent opening, size and position, wind speed and direction) and the crop transpiration (distribution of the irrigation) can easily be investigated and the different effects can be compared with respect to plant functioning and the solving of environmental problems, such as, losses of water and nitrogen in the environment.

References

- Bot, G.P.A., 1983. Greenhouse climate: from physical process to a dynamic model. Ph.D. Thesis, Agric. Univ. Wageningen, The Netherlands, pp. 240.
- Boulard, T., Baille, A., 1995. Modeling of air exchange rate in a greenhouse equipped with continuous roof vents. *J. Agric. Eng. Res.* 61, 37–48.
- Boulard, T., Draoui, B., 1995. Natural ventilation of a greenhouse with continuous roof vents: measurements and data analysis. *J. Agric. Eng. Res.* 61, 27–36.
- Boulard, T., Wang, S., 2000. Greenhouse crop transpiration simulation from external climate conditions. *Agric. For. Meteorol.* 100 (1), 25–34.

- Boulard, T., Meneses, J.F., Mermier, M., Papadakis, G., 1996. The mechanisms involved in the natural ventilation of greenhouses. *Agric. For. Meteorol.* 79, 61–77.
- Boulard, T., Papadakis, G., Kittas, C., Mermier, M., 1997. Air flow and associated sensible heat exchanges in a naturally ventilated greenhouse. *Agric. For. Meteorol.* 88, 111–119.
- Boulard, T., Lamrani, M.A., Roy, J.C., Jaffrin, A., Bouirden, L., 1998. Natural ventilation by thermal effect in a one-half scale model mono-span greenhouse. *Trans. ASAE* 41 (3), 773–781.
- Boulard, T., Wang, S., Haxaire, R., 2000. Mean and turbulent air flows and microclimatic patterns in a greenhouse tunnel. *Agric. For. Meteorol.* 100 (2–3), 169–181.
- Campbell, G.S., 1977. *An Introduction to Environmental Biophysics*. Springer, New York, p. 159.
- CFD2000 manual (v3.0), 1997. *Computational fluid dynamics systems*. Pacific Sierra Research Corporation, USA.
- de Halleux, D., Nijssens, J., Deltour, J., 1991. Adjustment and validation of a greenhouse climate dynamic model. *Bull. des Recherches Agronomiques de Gembloux* 26, 429–453.
- De Jong, T., 1990. *Natural ventilation of large multi-span greenhouses*. Ph.D. Thesis, Agric. Univ. Wageningen, The Netherlands, pp. 116.
- Fernandez, J.E., Bailey, B.J., 1992. Measurement and prediction of greenhouse ventilation rates. *Agric. For. Meteorol.* 58, 229–245.
- Haxaire, R., 1999. *Characterization and modelling of the airflow in a greenhouse*. Ph.D. Thesis, University of Nice Sophia Antipolis, France. pp. 149.
- Issa, R.I., 1985. Solution of the implicitly discretized fluid flow equations by operator-splitting. *J. Computat. Phy.* 62, 40–65.
- Jones, P.J., Whittle, G.E., 1992. Computational fluids dynamics for building air flow prediction-current capabilities. *Building Environ.* 27 (3), 321–338.
- Kacira, M., Short, T.H., Stowell, R.R., 1998. A CFD evaluation of naturally ventilated, multi-span, sawtooth greenhouses. *Trans. ASAE* 41 (3), 833–836.
- Kindelan, M., 1980. *Dynamic modelling of greenhouse environment*. *Trans. ASAE* 23, 1232–1239.
- Kittas, C., Draoui, B., Boulard, T., 1995. Quantification of the ventilation of a greenhouse with a roof opening. *Agric. For. Meteorol.* 77, 95–111.
- Lauder, B.E., Spalding, D.B., 1974. *The numerical computation of turbulent flows*. *Computat. Method Appl. Mechan. Eng.* 3, pp 269.
- Mistriotis, A., Bot, G.P.A., Picuno, P., Scarascia, G., 1997. Analysis of the efficiency of greenhouse ventilation using computational fluid dynamics. *Agric. For. Meteorol.* 85, 217–228.
- Mohammadi, B., Pironneau, O., 1994. *Analysis of the k-Epsilon Turbulence Model*. *Research in Applied Mathematics*. Wiley, Masson.
- Pollet, S., Bleyaert, P., Lemeur, R., 1999. Calculating the evapotranspiration of head lettuce by means of the Penman-Monteith Model. In: *3rd International Workshop: Model for plant growth and control of the shoot and root environment in greenhouses*. The Volcani Center, Bet Dagan, Israel, 21–25 February.
- Stanghellini, C., 1987. *Transpiration of greenhouse crops: an aid to climate management*. Ph.D. Thesis, Agric. Univ. Wageningen, The Netherlands, pp. 150.
- Wilson, J.D., 1985. Numerical studies of flow through a windbreak. *J. Wind Eng. Ind. Aerodynamics* 21, 119–154.
- Wang, S., Deltour, J., 1996. An experimental ventilation function for large greenhouses based on a dynamic energy balance model. *Agric. Eng. J.* 5, 103–112.
- Wang, S., Deltour, J., 1999. Airflow patterns and associated ventilation function in large scale multi-span greenhouses. *Trans. ASAE* 42 (5), 1409–1414.
- Wang, S., Boulard, T., 2000a. Predicting the microclimate in a naturally-ventilated plastic-house under Mediterranean climate. *J. Agric. Eng. Res.* 75, 27–38.
- Wang, S., Boulard, T., 2000b. Measurement and prediction of solar radiation distribution in full scale greenhouse tunnel. *Agronomie* 20, 41–50.
- Wang, S., Boulard, T., Haxaire, R., 1999. Air speed profiles in a naturally-ventilated greenhouse with a tomato crop. *Agric. For. Meteorol.* 96 (4), 181–188.
- Yang, X., Short, T.H., Fox, R.D., Bauerle, W.L., 1990. *Dynamic modelling of the microclimate of a greenhouse cucumber row-crop, Part II. Validation and simulation*. *Trans. ASAE* 33 (5), 1710–1716.